

Droplets atop a wrinkled substrate

Y Zhang, H Fan, W Huang, and Y Chen*

School of Mechanical and Aerospace Engineering, Nanyang Technological University, Singapore

The manuscript was received on 2 November 2009 and was accepted after revision for publication on 24 February 2010.

DOI: 10.1243/09544062JMES2069

Abstract: Liquid droplets atop both isotropically and anisotropically patterned substrate surfaces are investigated experimentally. The patterns are realized by means of elastic wrinkling/buckling of a thin layer of gold coated atop polystyrene shape memory polymer. Static contact angles are measured, and images showing the shapes of droplets are captured. The results obtained from isotropically patterned substrates suggest that surface roughness has no apparent effect on the static contact angles in this study. However, atop anisotropically patterned substrates, both the static contact angles and shapes of droplets vary with the direction of wrinkles and size of droplets.

Keywords: contact angle, patterned substrate surfaces, anisotropy, shape memory polymers

1 INTRODUCTION

Wetting and spreading are universal phenomena in nature and in our daily life. It leads to numerous applications in industry, such as printing and soldering [1–3]. Usually, it is studied by taking a liquid droplet atop a solid surface as an object [4], and the variables are related by Young equation (1) (Fig. 1). Regarding the influencing factors of such a wetting process, the properties of the solid surface are often studied by researchers. In recent years, with the development in micro-/nanotechnologies, various types of surface structures have been created. Among them, those with square-shaped pillars and parallel grooves or stripes [5] are extensively investigated, the latter of which provides an excellent model to study the wetting anisotropy

$$\gamma_{sg} = \gamma_s + \gamma_{gl} \cos \theta \quad (1)$$

where γ_{sg} , γ_s , and γ_{gl} are interfacial tensions between solid and gas, liquid and solid, and gas and liquid, respectively.

Besides the work done on the effects of solid surfaces, studies were also carried out to investigate the influence of liquid droplet properties such as viscosity and chemistry of the liquid material [6, 7]. However,

less attention was paid to another possible influencing factor, the droplet size. Many of the existing relevant studies have been employed as the method to experimentally determine the line tension as reviewed by Amirfazli and Neumann [8–12]. Regarding the investigations highlighting the droplet size effect on wetting and spreading, in 2003, Brandon *et al.* [13] reported their simulation work on the partial wetting on chemically heterogeneous substrates. Both contact angle hysteresis and droplet shape changes with the increase in droplet size were discussed. According to their results, the shape of larger droplets appeared to approach that of a spherical cap and the contact line was more circular in shape than that of smaller droplets. Recently, Bliznyuk *et al.* [14] also studied the evolution of droplet shape with the increase in droplet size when spreading on chemically stripe-patterned surfaces. However, the conclusion is merely based on the spreading on chemically heterogeneous surfaces. More studies are needed to systematically investigate the droplet size effect, such as extending the work to the spreading on topographically patterned surfaces.

In the present work, model substrates with structural patterns were designed and introduced to experimentally investigate the effects of both solid surface patterns and liquid droplet size. The system is confined by applying continuum physics as theoretically explained below.

In the viewpoint of continuum physics, the total energy of a condensed matter could be divided into the energy associated with volume (E_v) and that

*Corresponding author: School of Mechanical and Aerospace Engineering, Nanyang Technological University, 50 Nanyang Avenue, Singapore 639798, Singapore.
email: chenyan@ntu.edu.sg

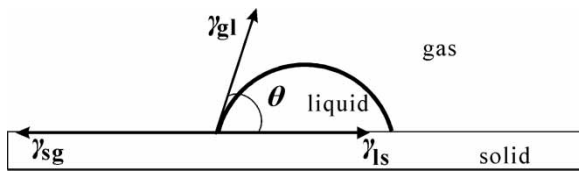


Fig. 1 Illustration of Young equation

associated with surfaces (E_s). For macroscopic liquid droplets, the energy associated with volume dominates its dynamic spreading process [15], whereas for sub-millimetre-sized liquid droplets, the energy associated with surfaces becomes dominant. The energy associated with volume could be represented by its gravity potential energy

$$E_v = mgR = \rho VgR = \frac{4\pi}{3}R^4\rho g \quad (2)$$

where R is the radius of the initial droplet and ρ is the density of the liquid.

The surface-related energy can be estimated as

$$E_s = 4\pi R^2\gamma \quad (3)$$

where γ is the surface tension of the liquid.

Substituting the physical constants of de-ionized (DI) water [16], surface tension $\gamma = 72 \times 10^{-3} \text{ J/m}^2$ and density $\rho = 1000 \text{ kg/m}^3$, into equations (2) and (3) and making the energies equal, a critical value of initial droplet radius is obtained, $R = 4.69 \text{ mm}$, which is sometimes called the capillary length [16, 17]. When the water droplet is much smaller than this critical size, the effects of gravity can be ignored, and the spreading process is driven by conversion among the surface energies. If the size of the water droplet is further reduced, such as 1 nm to $10 \mu\text{m}$ as discussed by Fan [16], the line tension will be comparable with surface tension and should be considered for predicting the droplet spreading.

In the present study, the radius of water droplets is in the millimetre or sub-millimetre scale, which is within the range that surface energies should dominate. Both isotropically and anisotropically patterned surfaces are fabricated by means of wrinkling/buckling of a thin layer of gold coated atop shape memory polymer (SMP). The surface patterns are reproducible, and the substrates can be reused. The influence of surface roughness, the droplet size, and the wetting anisotropy is examined.

2 EXPERIMENTAL DETAILS

2.1 Substrate preparation and characterization

The SMP sample used in the present study is thermo-responsive polystyrene SMP from Cornerstone

Research Group, USA. It is obtained by bulk random copolymerization. The as-received material is in sheet form with a thickness of about 3.5 mm , and no phase separation is found in the sheets. The glass transition temperature (T_g) of the SMP is about 65.5°C , as provided by the supplier and further verified by differential scanning calorimetry tests [18]. The method adopted for substrate preparation is the wrinkling/buckling process, which has been proven for the forming of highly ordered patterns [19–21].

To fabricate the substrates, the SMP samples were cut into rectangular and dumbbell shapes, and all of them were heated to 150°C before use to remove any possible residual stress or deformation during polymer processing. Subsequently, the samples were polished gently using Micropolish alumina compound ($0.3 \mu\text{m}$ and then $0.05 \mu\text{m}$; Buehler, USA) on DP-Nap cloth (Struers, Denmark). The average surface roughness of the resulted samples (R_a) was measured to be smaller than 20 nm using PL μ confocal imaging profiler (Sensofar-Tech, Spain). After this treatment, the samples were prepared for smooth, isotropically patterned, and anisotropically patterned substrates, respectively, according to the following procedures.

To prepare smooth substrates, the rectangular samples were coated with a thin layer of gold ($20\text{--}60 \text{ nm}$) by using a sputtering coater (SC7640 gold coater, Quorum Technologies, UK). To obtain different coating thicknesses, various coating times were applied. Empirically, the thickness of the gold layer was approximately proportional to the coating time.

To prepare isotropically patterned substrates, first, the rectangular samples were coated with a thin layer of gold ($20\text{--}60 \text{ nm}$). Secondly, they were heated at 150°C for 20 min and then cooled down to room temperature (22°C). After these procedures, isotropic patterns were created atop the substrate surfaces (Fig. 2). By depositing gold layers of different thicknesses, isotropically patterned substrates with different surface roughness can be prepared.

To prepare anisotropically patterned substrates, the dumbbell-shaped samples were first stretched to a certain tensile strain ($5\text{--}8 \text{ per cent}$) in a hot chamber at a temperature a bit higher than its T_g ($95\text{--}105^\circ\text{C}$). After extension, the samples were kept clamped on a stretching machine (Instron 5569, USA) to maintain the temporary shape when cooling down to room temperature. The loading and unloading processes are shown in Fig. 3. Then the samples were removed from the stretching machine. Finally, the stretched samples were coated with a thin layer of gold and heated at 120°C for 20 min . After cooling down to room temperature, the sample returned to its original length, and wrinkles were formed perpendicular to the stretching direction. In such a way, anisotropic patterns were realized atop the substrate surfaces (Fig. 4). By varying the conditions in which the SMP samples were processed, such as the temperature at which

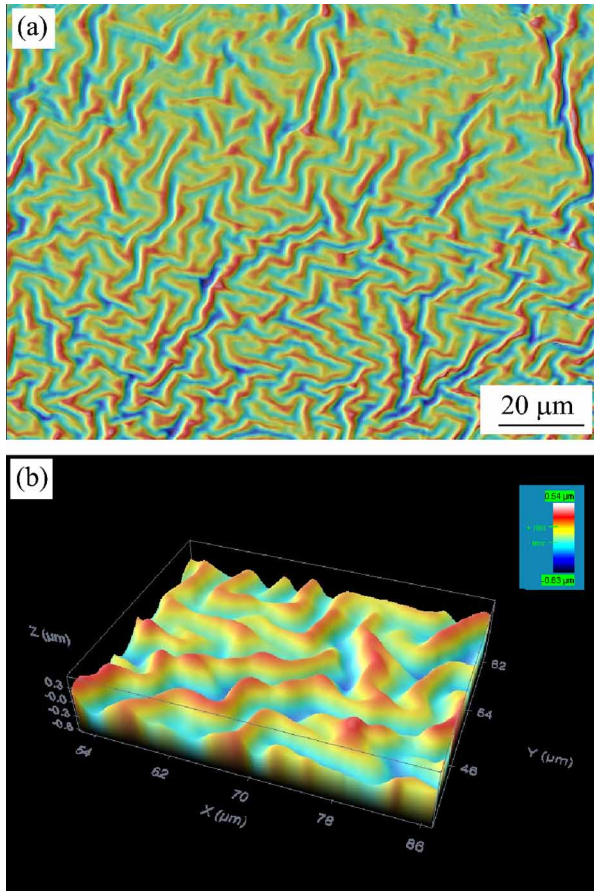


Fig. 2 Typical images of isotropically patterned substrates: (a) two-dimensional surface micrograph and (b) zoomed three-dimensional topography

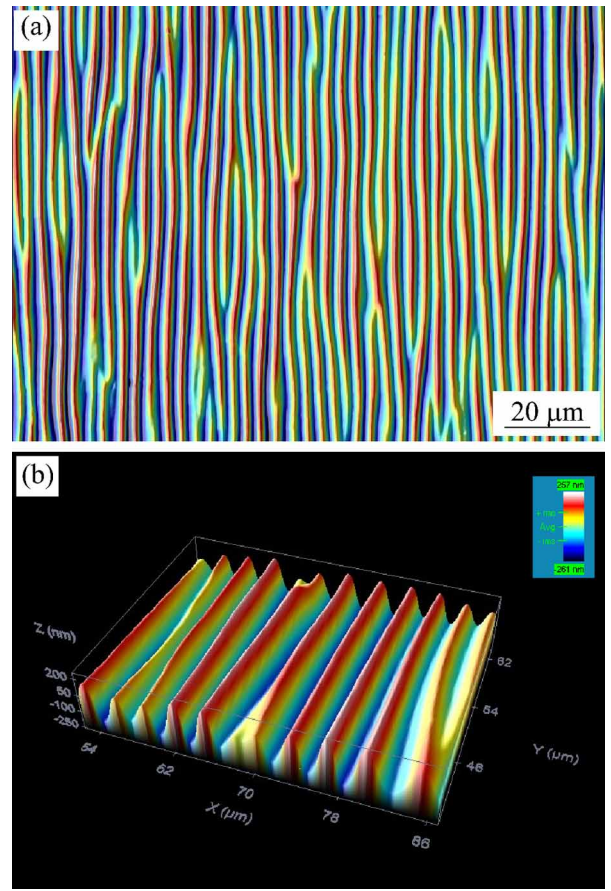


Fig. 4 Typical images of anisotropically patterned substrates: (a) two-dimensional surface micrograph and (b) zoomed three-dimensional topography

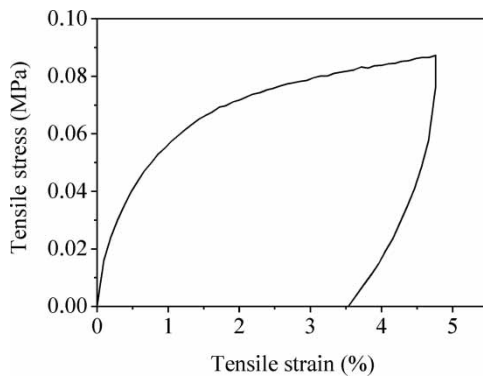


Fig. 3 Typical stress versus strain relationship in uniaxial stretching of the SMP sheet

they were stretched and the thickness of the coating layer, anisotropically patterned substrates with various surface roughness and wrinkle wavelength can be obtained.

After preparation, surface features of the substrates were characterized by a PLμ confocal imaging profiler; both surface roughness (R_a) and wrinkle wavelength (λ) were obtained.

2.2 Static contact angle measurement

To study wetting on such patterned substrates, the water droplets were gently placed onto the substrates using micropipettes, and front view images were taken using FTA 200 setup (First Ten Angstroms, USA) after a while when spreading reached its equilibrium state. The static contact angles and sessile droplet dimensions were measured using FTA 32 software (First Ten Angstroms). The static contact angles were measured at four points from two orthogonal directions. As for the smooth and the isotropically patterned substrates, as the values obtained from the two directions were similar, the four results were averaged to get the static contact angle. As for the anisotropically patterned substrates, the two directions are perpendicular (x -direction) and parallel (y -direction) to wrinkles, respectively. As illustrated in Fig. 5, contact angles θ_x and θ_y are the average values of the two angles measured at the contact points along x - and y -directions. Besides, top view images of the droplets were captured by a CCD camera (Leica DFC290, Germany) or a digital camera (Ricoh R6, Japan) to obtain the shapes of droplets after spreading. Spreading

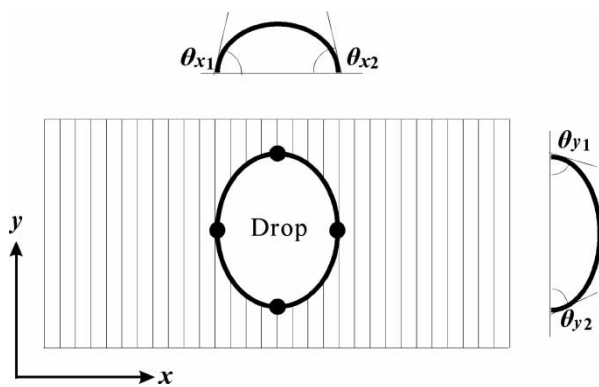


Fig. 5 Schematic drawing of droplet shape after spreading on anisotropically patterned substrates. The stretching is in the x -direction

on anisotropically patterned substrates with various surface rough profiles was studied and compared.

For all the substrates, water droplets with various volumes were tested. The volumes and the corresponding initial droplet radii are $0.5 \mu\text{l}$ ($R = 0.49 \text{ mm}$), $1 \mu\text{l}$ ($R = 0.62 \text{ mm}$), $3 \mu\text{l}$ ($R = 0.89 \text{ mm}$), $6 \mu\text{l}$ ($R = 1.13 \text{ mm}$), $12 \mu\text{l}$ ($R = 1.42 \text{ mm}$), and $20 \mu\text{l}$ ($R = 1.68 \text{ mm}$). They are much smaller than the capillary length for DI water. For each droplet size, atop each substrate, four measurements were carried out at different positions, and results were averaged to give the reported values.

3 RESULTS AND DISCUSSION

3.1 Patterns of substrate surfaces

After being heated to the temperature higher than its T_g , molecular chains of a polymer material became flexible and began to stretch in various directions, causing the SMP sample to expand to a larger size macroscopically. Once being cooled, the chains shrank to their original coil state and the SMP sample returned to its original shape. Isotropically patterned wrinkles were formed in this process owing to the mismatch of mechanical properties between the SMP sample and the coating film.

The surface roughness of the three smooth substrates and two isotropically patterned substrates is listed in Table 1. Different coating times were applied to the substrates, and various thicknesses of the coating layer resulted correspondingly. The relationship between wrinkle wavelength and coating thickness was in accordance with equation (4) as referred in some previous publications [19, 20, 22]

$$\lambda = 2\pi h \left[\frac{(1 - \nu_s^2)E_f}{3(1 - \nu_f^2)E_s} \right]^{1/3} \quad (4)$$

where h is the coating thickness, ν_s and E_s the Poisson ratio and the elastic modulus of the SMP sheet, and ν_f

Table 1 Surface roughness of smooth and isotropically patterned substrates

Substrates	Coating time (s)	R_a (μm)	λ (μm)
Smooth-1 (S1*)	200	0.016 ± 0.004	–
Smooth-2 (S2)	400	0.018 ± 0.003	–
Smooth-3 (S3)	600	0.016 ± 0.002	–
Isotropic-1 (I1)	120	0.115 ± 0.003	2.79 ± 0.29
Isotropic-2 (I2)	700	0.299 ± 0.023	17.10 ± 1.79

*Labels apply in the following discussions and figures.

Table 2 Surface roughness and wrinkle wavelength of anisotropically patterned substrates

Substrates	R_a (μm)	λ (μm)
Anisotropic-1 (A1*)	0.113 ± 0.007	4.09 ± 0.24
Anisotropic-2 (A2)	0.253 ± 0.003	7.04 ± 0.61
Anisotropic-3 (A3)	0.292 ± 0.016	12.54 ± 1.07

*Labels apply in the following discussions and figures.

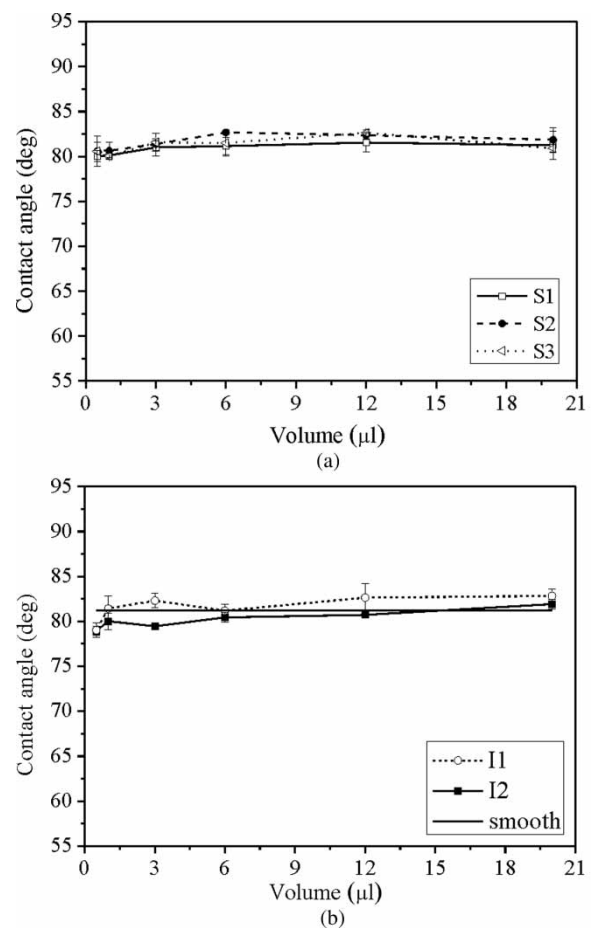


Fig. 6 Static contact angles measured atop (a) smooth and (b) isotropically patterned substrates. The value for the benchmark line in (b) is 81.2° , obtained by averaging all the contact angles measured atop smooth substrates

and E_f are the Poisson ratio and the elastic modulus of the coating film.

As for anisotropically patterned substrates, they were stretched in one direction at a temperature higher than their T_g , and the temporary shapes were frozen when cooling down on the clamps. However,

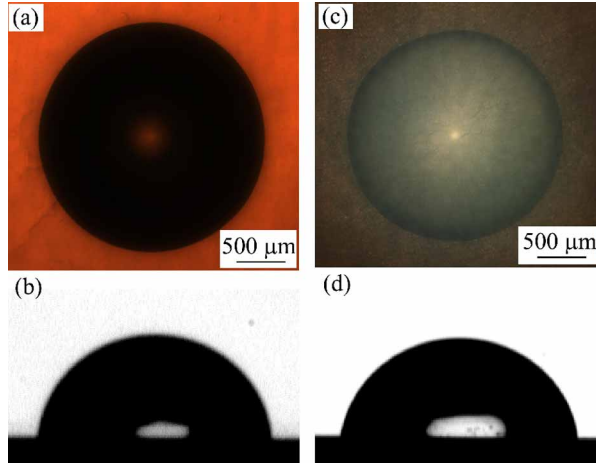


Fig. 7 Microscopic images of droplets (3 μ l) atop (a and b) smooth substrates (S2) and (c and d) isotropically patterned substrates (I1). (a, c) Top view and (b, d) front view

the original shape of the sample had been memorized by the material as the permanent shape. Once it was heated again, the molecular chains became flexible and intended to return to their original coil state, which was entropy-high. Therefore, when cooling down, the stretched substrate retracted in the extension direction and went back to its original shape, resulting in parallel wrinkles perpendicular to the stretching direction.

To prepare the anisotropically patterned substrates with various wrinkle profiles, parameters were varied as described in section 2.1. Similar to the case for the isotropically patterned substrates, wavelength increased with coating thickness. Besides, the temperature at which the SMP samples were stretched also had influence on the wavelength. This may be explained by the relationship between the elastic modulus of SMP and the temperature. The decrease in the modulus of SMP with an increase in temperature leads to larger wavelength, according to equation (4). In addition, the residual strain after releasing the tensile stress takes effect in tuning the wrinkle wavelength (Fig. 3). The three anisotropically patterned substrates selected for spreading experiments are listed in Table 2.

As the polymer material used for the preparation of solid substrates is a kind of SMP and the coating

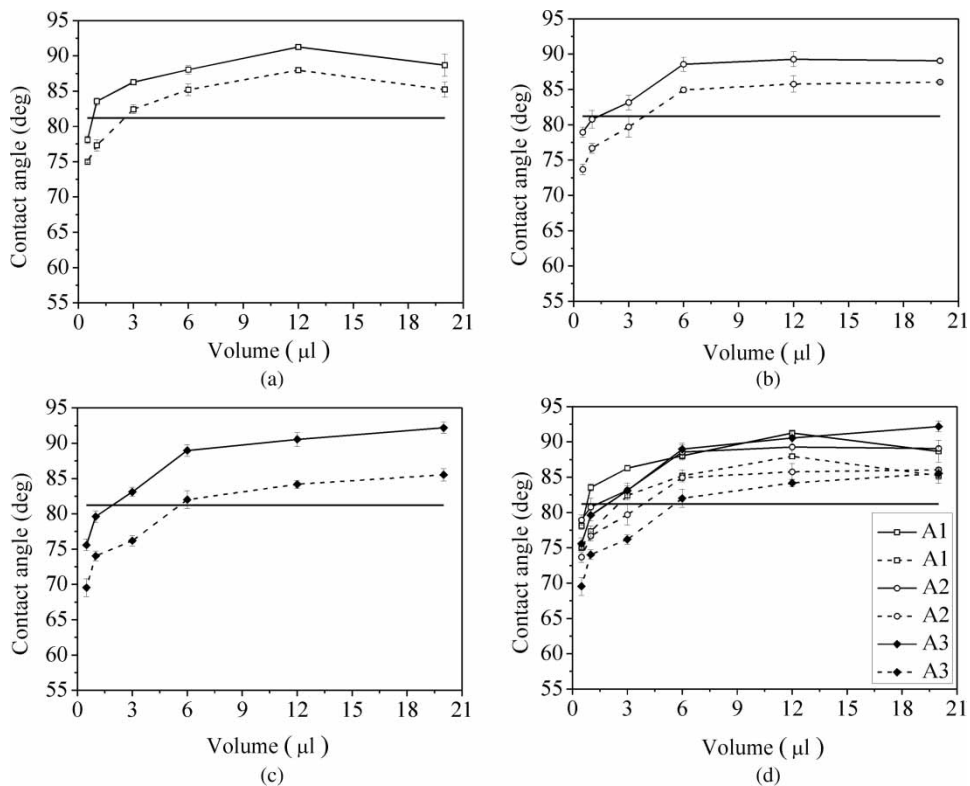


Fig. 8 Static contact angles measured atop anisotropically patterned substrates: (a) atop the substrate A1; (b) atop the substrate A2; (c) atop the substrate A3; and (d) comparison among the three substrates. θ_x is guided in solid line and θ_y dashed line

film is as thin as several tens of nanometres, the substrates can be reused after removing the patterned layer through polishing and retaining their original shapes through heat treatment. Besides, as the pattern profiles could be controlled by quantitatively adjusting the preparation conditions, the resulted substrates are reproducible and reusable, which is favourable in the investigation of the spreading phenomenon.

3.2 Spreading on smooth substrates

The measured static contact angles of droplets with six different sizes atop the three smooth substrates are summarized in Fig. 6(a). It shows that the droplet size has no effect on the static contact angles, which agrees well with the theoretical predictions stated in section 1. Besides, the results are comparable with those reported by Cognard [23]. Microscopic images (Fig. 7(a)) indicate that the three-phase contact line atop smooth substrates is circular. In addition, front view observation (Fig. 7(b)) shows that the droplet almost keeps in a spherical cap after reaching the equilibrium state.

The nearly overlapped lines in Fig. 6(a) suggest no influence of coating thickness on the static contact angles. This conclusion implies that when considering wetting on the isotropically and anisotropically patterned substrates, there is no need to take the coating thickness itself into consideration. The authors can only concentrate on the resulted roughness and wavelength no matter what coating time is applied.

3.3 Spreading on isotropically patterned substrates

The static contact angles were measured atop two isotropically patterned substrates, and the results were compared with the average value obtained atop smooth substrates. Figure 6(b) shows that there is also no droplet size effect on isotropically patterned substrates. Figures 7(c) and (d) show that the droplet atop such substrates is a spherical cap with a circular contact line, which is similar to that atop smooth substrates.

Regarding the influence of surface roughness on static contact angles, the Wenzel equation (5) [24] is adopted to explain the experimental results

$$\cos \theta_W = r \cos \theta \quad (5)$$

where θ_W is the apparent contact angle on the rough surface and r , the roughness factor, is the ratio of the true solid area to the planar projection area.

By computing the true solid area and the planar area of the isotropically patterned surfaces from the raw data obtained from a confocal imaging profiler, the roughness factor was estimated to be around 1.01 for the two isotropically patterned substrates. R_a as

small as $0.3 \mu\text{m}$ and such a small r lead to little effect of surface roughness on the static contact angles. The experimentally measured contact angles on the isotropically patterned substrates were very close to those on smooth substrates. Theoretically, 2° difference between θ_W and θ needs r to be 1.2, which is much larger than that in the present study. The small roughness factor may be explained by the aspect ratio of the patterned surfaces. When the water droplet was placed atop the solid substrate, the radius of the droplet-covered area was in the millimetre scale, whereas the height of wrinkles was in the nanometre scale, thus globally, the surfaces were not very rough.

3.4 Spreading on anisotropically patterned substrates

When a water droplet was placed atop an anisotropically patterned substrate, it would spread more in the direction parallel to wrinkles (y -direction), and the contact angles are different between the directions parallel and perpendicular to wrinkles. $\Delta\theta = \theta_x - \theta_y$ is the measure of wetting anisotropy (refer to Fig. 5 for the meaning of θ_x and θ_y). Meanwhile, as the

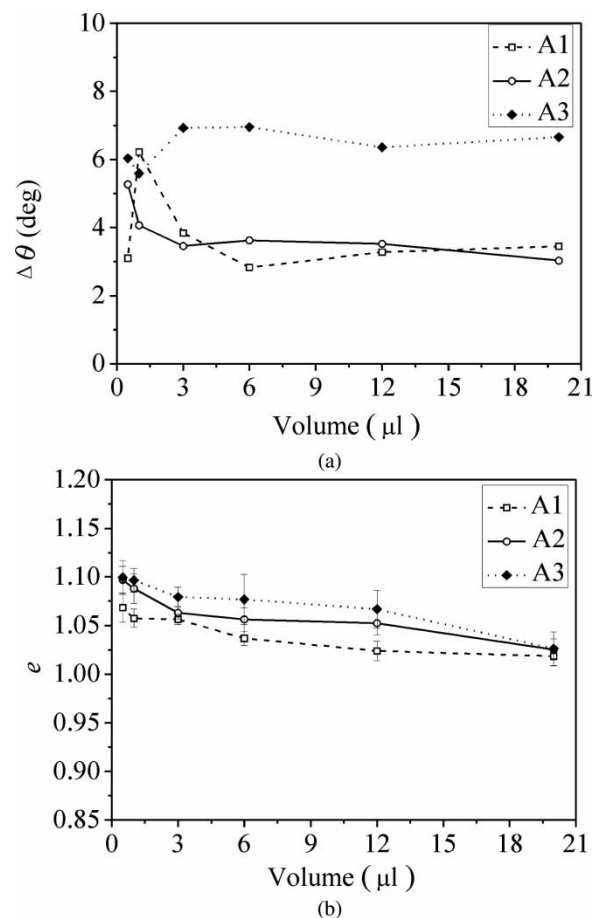


Fig. 9 (a) Contact angle difference and (b) droplet elongation atop anisotropically patterned substrates

water droplet elongates along wrinkles (y -direction), the droplet elongation, $e = L_y/L_x$, can serve as another measure of wetting anisotropy, where L_y is the axial length of the droplet along wrinkles and L_x is the axial length of the droplet perpendicular to wrinkles.

Measured static contact angles atop the three anisotropically patterned substrates are plotted in Fig. 8. Different from the cases of smooth and isotropically patterned substrates, the contact angles in both directions (θ_x and θ_y) increased with the droplet size. However, the results cannot be simply explained by either Wenzel equation or Cassie model [25].

The roughness factor of the three anisotropically patterned substrates is calculated to be in the range of 1.02–1.05, which would result in the apparent contact angle around 81° and show little effect of surface roughness. If computing by applying the Cassie model, apparent contact angle as large as 170° could be expected when the droplets are on anisotropically patterned surfaces with air being trapped between wrinkles. However, even for the largest droplet and the most rough surface studied, the measured contact angle did not exceed 100° , which implies that the

Cassie state cannot be the dominating mode in this wetting phenomenon. The larger value of θ_x may be the results of wetting anisotropy.

$\Delta\theta$ and e for the three substrates at various droplet sizes were calculated and compared, as shown in Fig. 9. A bigger $\Delta\theta$ or e represents a more obvious anisotropy effect. Although there was no clear relationship between $\Delta\theta$ and droplet size (Fig. 9(a)), e decreased with droplet size, as shown in Fig. 9(b). It reveals that the pattern anisotropy has a larger effect on the shape change of smaller droplets. As for the biggest droplet of the volume $20\ \mu\text{l}$, there was the least droplet distortion, although $\Delta\theta$ was still noticeable. Similar results were obtained by Bliznyuk *et al.* [14], although their experiments were carried out on chemically stripe-patterned surfaces. Moreover, the results also show that both $\Delta\theta$ and e have the highest value atop the substrate with the largest wrinkle wavelength (A3) for the same droplet size (Fig. 9), indicating the strongest wetting anisotropy.

Atop such anisotropically patterned substrates, the contact line of droplets is non-circular. The wrinkles allow water droplets to preferentially spread along

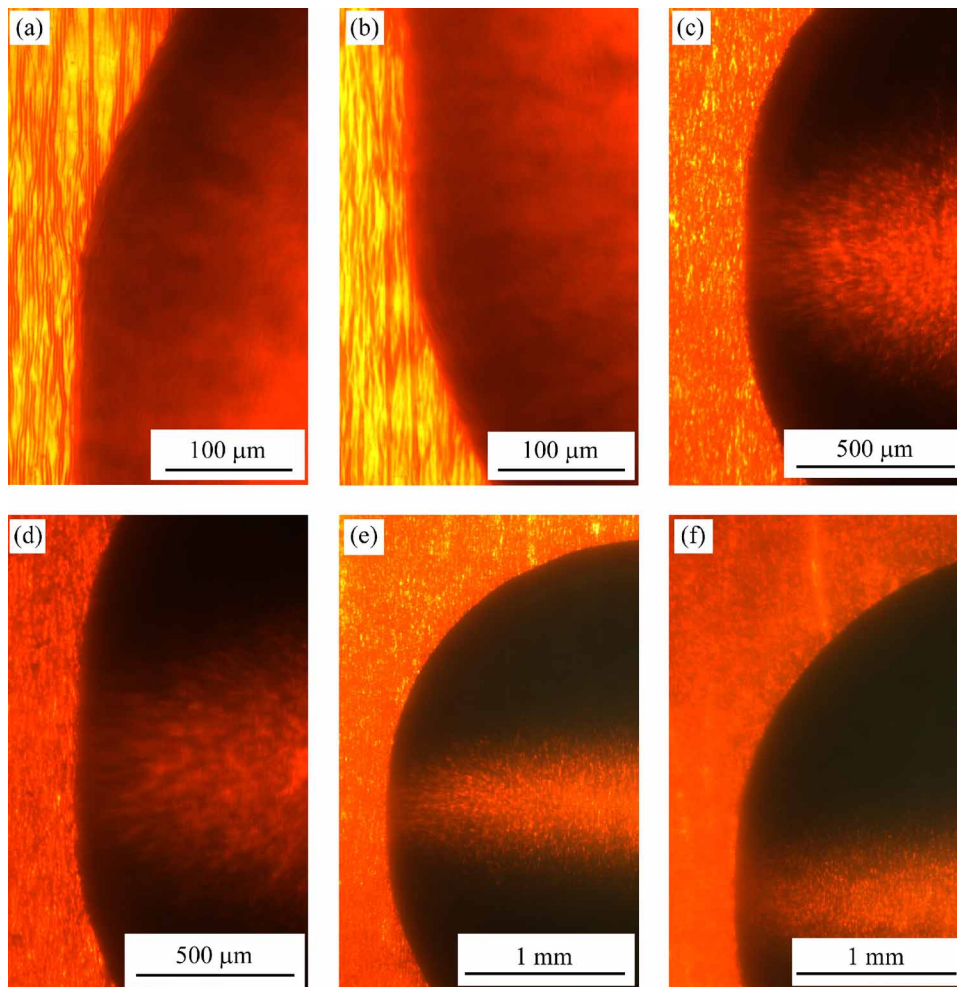


Fig. 10 Typical microscopic images highlighting the droplet edges pinned by wrinkles on substrate A2: (a) $0.5\ \mu\text{l}$; (b) $1\ \mu\text{l}$; (c) $3\ \mu\text{l}$; (d) $6\ \mu\text{l}$; (e) $12\ \mu\text{l}$; and (f) $20\ \mu\text{l}$

them, which requires a lower energy barrier. In addition, the droplet distortion might be attributed to the difference in wetting energy barrier between directions parallel and perpendicular to wrinkles [22]. The droplet is pinned when spreading perpendicular to wrinkles, and the bigger values of θ_x resulted from the pinning. Figure 10 shows the pinned edges when spreading perpendicular to wrinkles, and it was observed that the shape of the edge is much like part of a circle when spreading along wrinkles. There is an obvious transition between the two edges. However, not all the droplets of different sizes are pinned to the same extent. With the increase in the droplet size, the pinning is less obvious, as shown in Fig. 10. When the droplet is 20 μl , the edge parallel to wrinkles is not as straight as that of the smaller droplets any more, although it is still apparently not part of a circle.

4 CONCLUSIONS

Wrinkling/buckling is proven to be an effective method to fabricate both isotropically and anisotropically patterned substrates, the roughness factor of which is relatively low. Water droplet spreading phenomenon is studied experimentally atop smooth and patterned substrates. The influence of both solid surface patterns and liquid droplet size is investigated.

The surface roughness almost has no influence on the static contact angles when R_a is smaller than 0.3 μm and r is lower than 1.2 in the present experiments. Wetting anisotropy appears when spreading on the anisotropically patterned substrates: the static contact angles measured in the direction parallel to wrinkles are smaller than those measured in the direction perpendicular to wrinkles for the same droplet size; droplet elongates along wrinkles. The droplet size only has effect on the anisotropically patterned substrates: the static contact angles increase and the droplet elongation decreases with the increase in the droplet size. Besides, droplets would be pinned at the edges of wrinkles when spreading perpendicular to them, showing a non-circular shape, and the pinning is less obvious when the droplet is as large as 20 μl .

The authors could conclude that wetting and spreading behaviours could be more flexibly tuned by considering the influence of both solid surface patterns and liquid droplet properties. With the theoretical challenges and industrial application potentials, this should be a topic that warrants further investigations.

© Authors 2010

REFERENCES

- 1 Sharpe, R. B. A., Burdinski, D., Huskens, J., Zandvliet, H. J. W., Reinhoudt, D. N., and Poelsema, B. Spreading of 16-mercaptohexadecanoic acid in microcontact printing. *Langmuir*, 2004, **20**, 8646–8651.
- 2 Yang, Y.-S., Kim, H.-Y., and Chun, J.-H. Spreading and solidification of a molten microdrop in the solder jet bumping process. *IEEE Trans. Compon. Packag. Technol.*, 2003, **26**, 215–221.
- 3 Kim, C., Kang, S. C., and Baldwin, D. F. Experimental evaluation of wetting dynamics models for Sn₆₃Pb₃₇ and SnAg_{4.0}Cu_{0.5} solder materials. *J. Appl. Phys.*, 2008, **104**, 033537. pp. 1–13.
- 4 Yang, A.-S., Yang, M.-T., and Hong, M.-C. Numerical study for the impact of liquid droplets on solid surfaces. *Proc. IMechE, Part C: J. Mechanical Engineering Science*, 2007, **221**, 293–301. DOI: 10.1243/0954406JMES488.
- 5 Yoshimitsu, Z., Nakajima, A., Watanabe, T., and Hashimoto, K. Effects of surface structure on the hydrophobicity and sliding behavior of water droplets. *Langmuir*, 2002, **18**, 5818–5822.
- 6 Morita, M., Koga, T., Otsuka, H., and Takahara, A. Macroscopic-wetting anisotropy on the line-patterned surface of fluoroalkylsilane monolayers. *Langmuir*, 2005, **21**, 911–918.
- 7 Prabhu, K. N., Fernades, P., and Kumar, G. Effect of substrate roughness on wetting behaviour of vegetable oils. *Mater. Des.*, 2009, **30**, 297–305.
- 8 Drelich, J. The effect of drop (bubble) size on contact angle at solid surfaces. *J. Adhes.*, 1997, **63**, 31–51.
- 9 Drelich, J., Miller, J. D., and Hupka, J. The effect of drop size on contact angle over a wide range of drop volumes. *J. Colloid Interf. Sci.*, 1993, **155**, 379–385.
- 10 Drelich, J., Miller, J. D., Kumar, A., and Whitesides, G. M. Wetting characteristics of liquid drops at heterogeneous surfaces. *Colloids Surf. A Physicochem. Eng. Asp.*, 1994, **93**, 1–13.
- 11 Drelich, J., Miller, J. D., and Good, R. J. The effect of drop (bubble) size on advancing and receding contact angles for heterogeneous and rough solid surfaces as observed with sessile-drop and captive-bubble techniques. *J. Colloid Interf. Sci.*, 1996, **179**, 37–50.
- 12 Amirfazli, A. and Neumann, A. W. Status of the three-phase line tension. *Adv. Colloid Interf. Sci.*, 2004, **110**, 121–141.
- 13 Brandon, S., Haimovich, N., Yeger, E., and Marmur, A. Partial wetting of chemically patterned surfaces: the effect of drop size. *J. Colloid Interf. Sci.*, 2003, **263**, 237–243.
- 14 Bliznyuk, O., Vereshchagina, E., Kooij, E. S., and Poelsema, B. Scaling of anisotropic droplet shapes on chemically stripe-patterned surfaces. *Phys. Rev. E*, 2009, **79**, 041601. pp. 1–6.
- 15 Shikhmurzaev, Y. Moving contact lines in liquid/liquid/solid systems. *J. Fluid Mech.*, 1997, **334**, 211–249.
- 16 Fan, H. Liquid droplet spreading with line tension effect. *J. Phys. Condens. Matter*, 2006, **18**, 4481–4488.
- 17 Xu, L., Fan, H., Yang, C., and Huang, W. M. Contact line mobility in liquid droplet spreading on rough surface. *J. Colloid Interf. Sci.*, 2008, **323**, 126–132.
- 18 Liu, N., Huang, W. M., Phee, S. J., and Tong, T. H. The formation of micro-protrusions atop a thermo-responsive shape memory polymer. *Smart Mater. Struct.*, 2008, **17**, 057001. pp. 1–6.

- 19 Volynskii, A. L., Bazhenov, S., Lebedeva, O. V., and Bakeev, N. F. Mechanical buckling instability of thin coatings deposited on soft polymer substrates. *J. Mater. Sci.*, 2000, **35**, 547–554.
- 20 Genzer, J. and Groenewold, J. Soft matter with hard skin: from skin wrinkles to templating and material characterization. *Soft Matter*, 2006, **2**, 310–323.
- 21 Bowden, N., Brittain, S., Evans, A. G., Hutchinson, J. W., and Whitesides, G. M. Spontaneous formation of ordered structures in thin films of metals supported on an elastomeric polymer. *Nature*, 1998, **393**, 146–149.
- 22 Chung, J. Y., Youngblood, J. P., and Stafford, C. M. Anisotropic wetting on tunable micro-wrinkled surfaces. *Soft Matter*, 2007, **3**, 1163–1169.
- 23 Cognard, J. Adhesion to gold: a review. *Gold Bull.*, 1984, **17**, 131–139.
- 24 Wenzel, R. N. Resistance of solid surfaces to wetting by water. *Ind. Eng. Chem.*, 1936, **28**, 988–994.
- 25 Cassie, A. B. D. and Baxter, S. Wettability of porous surfaces. *Trans. Faraday Soc.*, 1944, **40**, 546–551.